Current Trends in Neurology
Vol. 14, 2020

Original Article

Multiplex signal transmission by spike waves (Part 1): Simulations

Shinichi Tamura*

Department of Radiology, Graduate School of Medicine, Osaka University, 2-2 Yamadaoka, Suita City, Osaka 565-0871, Japan.

ABSTRACT

It is unclear how neurons with variable response properties and stochastic failures can reliably transmit and process information. This article examines signal transmission and communication in the neural networks as an intermediate function of neural networks between artificial intelligence (AI) and each neuron functions, and derives multiplex signal transmission principle by spike waves in the neural networks. This article (Part 1) presents simulations of a two-dimensional (2D) mesh artificial neural network. If one of the transmitting neuron groups is stimulated, the signal is propagated in the form of spike waves with fluctuations. The corresponding receiving neuron group can identify the signal after learning to form an asynchronous multiplex communication channels such as 9:9 in the simulation. The communication channel is composed of many intermediate neurons working as relays. Each neuron can work as an input/output (I/O) and as a relay element, i.e., as a multiuse unit. Grouping and synchronic firing is often observed in real neuronal networks and appears to be effective for stable and robust spatial multiplex communication. This multiplex communication pattern is similar to that of sound identification by the ears and mobile adaptive communication systems. Some of the experimental results validating the simulation model and connecting it to wet experiments of the succeeding article (Part 2) using cultured neuronal network including spike code flow which shows part of spike waves, effects of using extracellular electrode, and an example of communication channels of 3:n in real cultured neuronal networks are also described. The results of both artificial neural network simulations (this Part 1) and multichannel recording of cultured neuronal networks (Part 2) support multiplex communication principle in the brain.

KEYWORDS: natural neural network, multiplex communication, learning, spike wave, fluctuation of neuron characteristics, relay neuron.

1. INTRODUCTION

Individual neurons within neuronal networks communicate through action potential (spike) trains with highly variable kinetics (length, mean frequency, and temporal change in frequency or accommodation). These properties are determined by synaptic connectivity patterns, individual synaptic strengths, and the biophysical properties (excitability) of individual neurons, all of which are dynamically modulated by various neurochemical signaling and plasticity mechanisms. However, it is difficult to determine how the spike trains are encoded and recognized by receiving neurons for reliable communication. Furthermore, compared to artificial elements such as transistors, neurons process spike information slowly (over milliseconds) and are not fully reliably (i.e., are prone to spike failure).

The present state of the art concerning the functional analysis of neural networks includes

*Email id: tamuras@nblmt.jp

(A) research on spike coding metrics [1], (B) spatiotemporal coding [2-6], (C) synfire chains [7-11], and (D) pseudo-random code analysis [12]. However, these analyses are generally not concerned with communication but rather with the firing behavior of the network. Thus, the basic properties of inter-neuronal communication remain to be elucidated. In cultured neuronal networks, various random-appearing spike trains are observed. Further, neurons in close proximity tend to fire in synchrony. However, to date, there is no satisfactory explanation on how these phenomena contribute to reliable communication. The aim of this paper is to derive the basic principles of communication in simple two-dimensional (2D) neural networks with fluctuating characteristics using a simulation protocol that corresponds to the activity profile of a real cultured neuronal network. Previous studies have implemented multiplex communication by cross bar-type switching in integrated circuit neural networks [13-15]. However, these are artificial hardware models that work synchronously without fluctuations. In these networks, links are established along a selected line, yielding point-to-point connections. By contrast, in this article, we[1] analyzed a simple 2D cultured neural network composed of more realistic asynchronous neurons with synapses that show temporal fluctuations. These analyses revealed a multiplex communication principle inherent to real neuronal networks based on propagation of spikes[2].

Figure 1 shows a time-shift diagram of 10.2 Hz magnetoencephalography (MEG) obtained in a previous study [16, 17] that provides a graphic illustration of the complex communication in the human brain. Note that every part of the brain can communicate with every other part *via* direct or indirect routes, similar to human societies that utilize multi-access communication tools. Therefore, we have previously proposed synchronous multiplex communication models for neural networks [18, 19]. However, synchronous actions are not realistic in real neuronal networks.

To investigate the mechanism of asynchronous information flow, we performed computer simulations using a 2D mesh-type neural network and observed the spatiotemporal properties of induced spike waves. These simulations confirmed that a network composed of integrate-and-fire model neurons without leakage but with fluctuating refractory periods and output delays provides a reasonable model of spike train propagation observed in real cultured neural networks [20, 21]. We first extracted natural spike code spectra [20] by recording spike trains from multiple electrodes within the cultured neuronal network and then extracted code spectra from 2D mesh-type neural network simulations [21]. By comparing these code spectra, we estimated the average characteristics of the refractory period (accepting period) and the output delay of cultured neurons. Further, this comparison confirmed that the integrate-and-fire neuron model without leakage provides a reasonable approximation of neuronal behavior as shown in Subsection 4.12 of Section 4.

We have also previously shown preliminarily that in a neural communication network, in spite of the fluctuating characteristics of the neurons, remote receiving neurons can determine the currently receiving spike trains come from which stimulated source neurons. The classification was made by using an external back propagation neural network (BPN) classification method [22]. In these simulations, almost all neurons of the network are employed as common relay media for multiplex communication. Further, as shown in Subsection 4.12.7 of Section 4 and the succeeding article (Part 2) (hereafter simply referred as “Part 2”) [23], 2:1 (or 2:2) communication and possibly even 3:1 (or 3:3) communication are possible in cultured neuronal networks using the dynamic time warping (DTW) method, interval matching

[1]The results in this article are obtained with support of those listed in the ‘ACKNOWLEDGEMENTS’ section.

[2]This work is presented in two parts, Part 1 and Part 2. Part 1 (current article) explains mainly about simulations and Part 2 (the succeeding article [23]) explains wet lab experiments. It is also an important feature of this research, that each wet lab experiment corresponds to the simulations and vice versa.

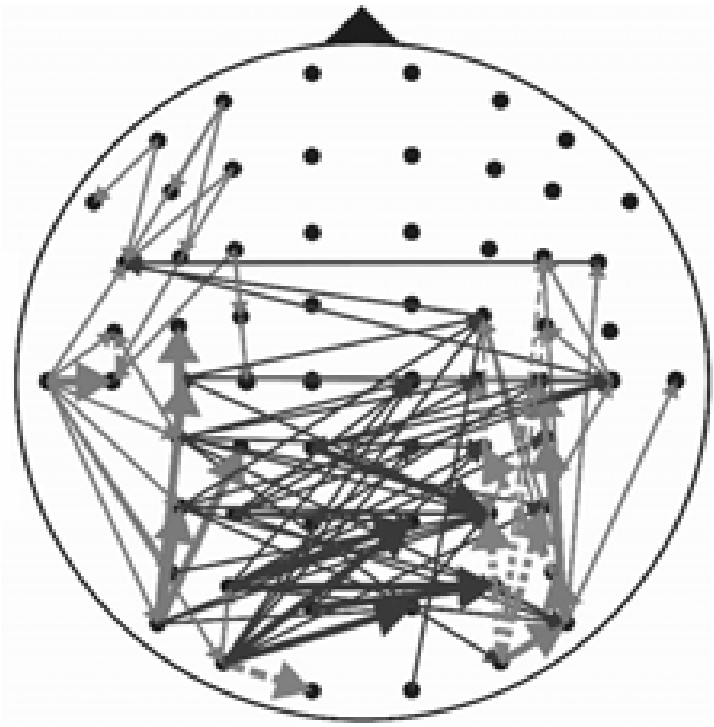

Figure 1. Time-shift map of 10.2 Hz MEG, for a number counting task. Gray: lag time < 5 [ms] within each hemisphere. Black: lag time > 10 [ms] mainly across the callosum. Dotted gray: lag time 5-10 [ms]. This example shows wide-range neural communication. The communication examined in this chapter is more local and occurs in a homogeneous neural network (a cultured neuronal network) [Clinical data].

method, and BPN [24-26]. To assess these principles in real neuronal networks, evoked spikes were recorded using an extracellular multi-electrode system with 64 (8 × 8) individual electrodes. Over each electrode, there appeared to be zero, one, or a few neurons. Stimulations were delivered by one of two electrodes ("1" and "2"), and we investigated which non-stimulating electrodes (=64-2=62) could identify "1" or "2" correctly using DTW, our original learning process, or BPN specifically for 2:1 or 2:2 communication channels. The non-stimulating electrodes collect spikes from neighboring receiving neurons. Best results showed that 52% (=32/62) of non-stimulating electrodes could identify the stimulating electrode with significant accuracy (Subsection 4.12.7 of Section 4), whereas others demonstrated less than significant accuracy or no response. We also indirectly demonstrated identification in 3:1 or 3:3 communication channels by combining 2:1 communication channels.

Tamura *et al*. [22] used BPN for a similar identification process in an artificial neural network. However, because BPN is not fully plausible in real neuronal networks, we applied a more simple series of temporal Laplacian–Gaussian (LG) filters, in Section 2, that have a learning function and behavior analogous to real neuronal networks. In Section 3, we present experimental results of a simulation showing that multiplex communication can be established in a neural network despite fluctuations in individual neuron characteristics. In Sections 4 and 5, we discuss our results and present our conclusions.

2. MATERIALS AND METHODS

2.1. Multiplex communication in artificial networks

We used a 25 × 25 2D mesh-type neural network with directional random weights assigned to the connections from and to eight neighboring neurons in each trial (Figure 2).

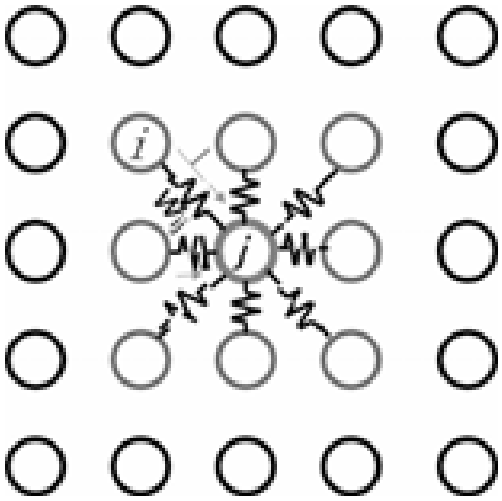

Figure 2. 2D mesh-type neural network with a simple flat structure, where spikes are inputted to neuron j asynchronously from eight neighboring neurons $\{i\}$.

2.1.1. Network configuration

There are many possible communication channel types in neural networks, such as C:1 and C:C (Figure 3). In this article, we examined C:C type communication channels because establishing C:C communication channels requires establishing C:1.

In our fluctuation model, the instantaneous output delay and accepting period values of each neuron during each firing event k deviate as described previously [27].

2.1.2. Stimulation

Stimuli are delivered at time t to the transmitting neuron s_{ij} belonging to group s_i, which is composed of three neurons: s_{i1}, s_{i2}, and s_{i3} (Figure 4). Grouping was used based on preliminary findings that it improved the accuracy of communication [22]. Let $f_n(t)$ be an excitation function such that

$$f_n(t) = 1 \text{ if neuron } n \text{ fires at time } t, \text{ where } n = 1, 2, \ldots, 625, t = 1, 2, \ldots, 200, \quad (1)$$

$$0 \text{ otherwise.}$$

However, for simplicity, all initial stimuli are delivered at time 1 for individual training of each channel. In case of channel i, the spikes transmitted from neuron group $s_i = \{s_{i1}, s_{i2}, s_{i3}\}$ as the initial stimuli are expressed by

$$f s_{ij}(1) = 1; j = 1, 2, 3 \quad (2)$$

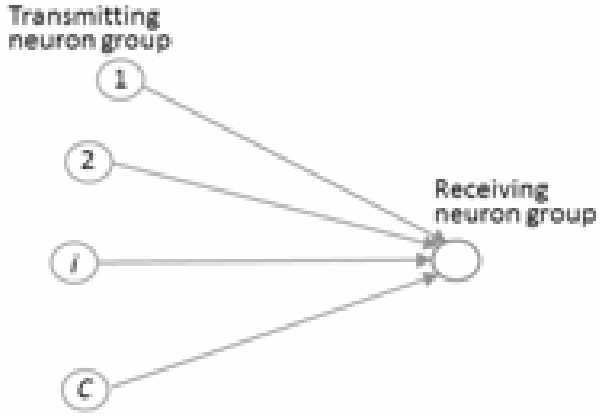

(a) C:1

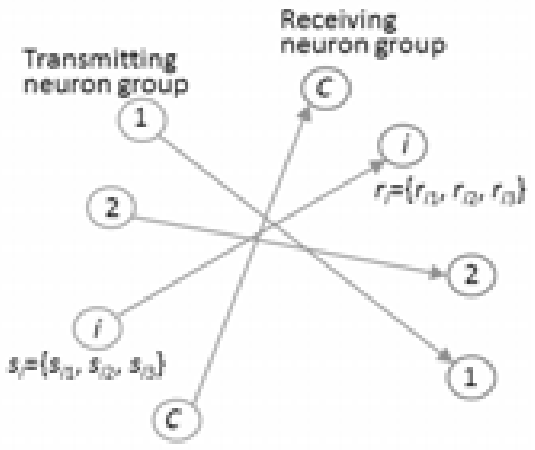

(b) C:C

Figure 3. Communication channel types. We assessed only the C:C type (b) for C = 3, 6, and 9 (i.e., 3:3, 6:6, and 9:9 communication channels). Each neuron group is composed of three neurons.

and are equal to zero otherwise. Stimuli are propagated in the network as spike waves as shown in Figure 5.

The 2:2 multiplex communication by spike waves is shown in Figure 6. If the receiving neuron group A' can identify the stimulation from A correctly, and B' can identify the stimulation from B correctly, the communication channels are regarded as established.

2.1.3. Calculation for detection and communication

The receiving mechanism is a kind of pattern recognition, and there are several possible methods

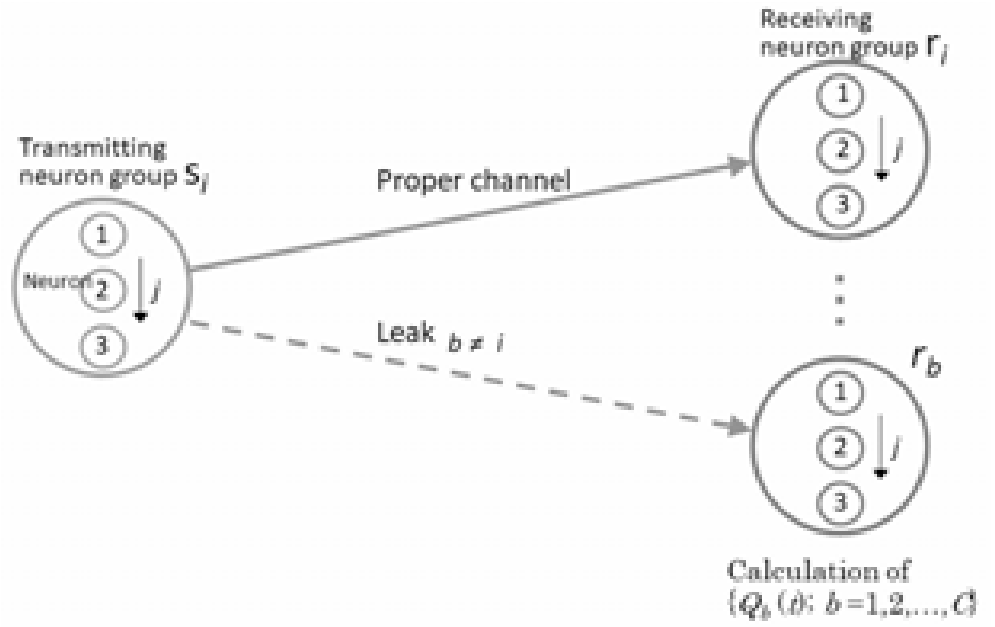

Figure 4. Neuron groups and communication channel.
$i, b \in \{1, 2,\ldots, C\}, j \in \{1, 2, 3\}$.

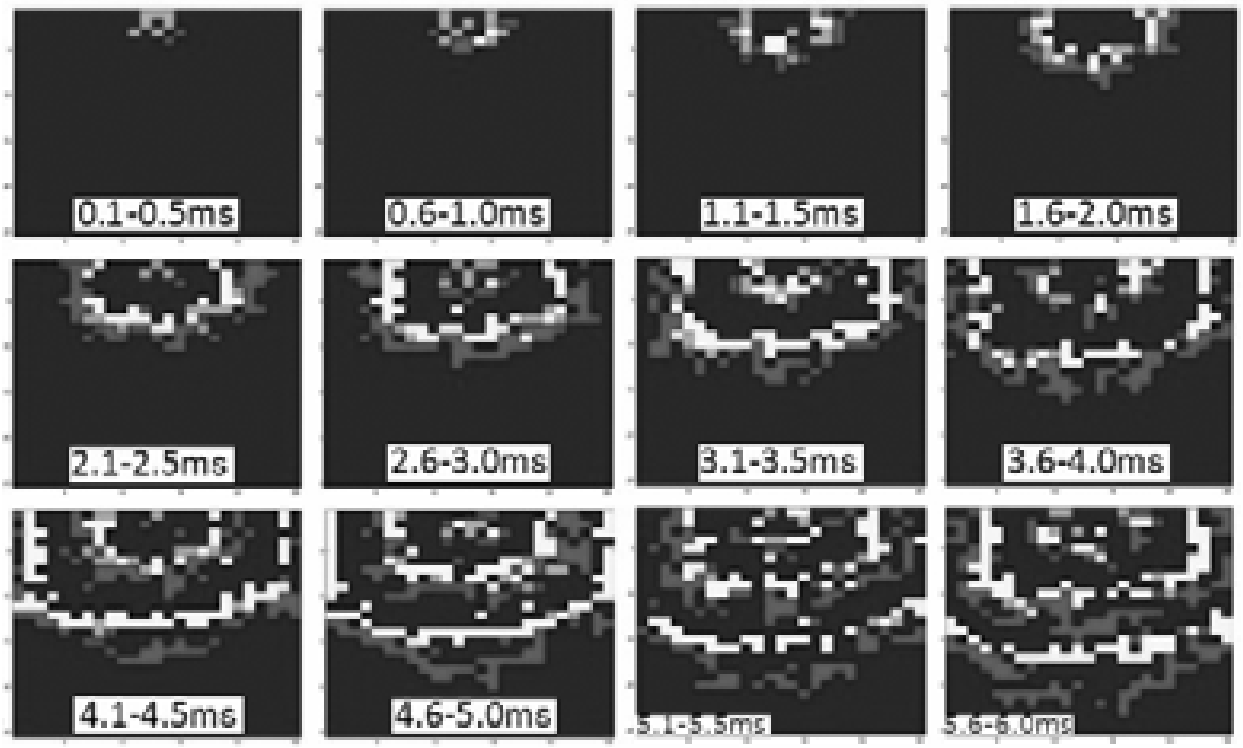

Figure 5. Spike waves between 0.1 and 5.0 ms in a 25 × 25 network after the three top center neurons are stimulated. White indicates firing cells where $F_{OD} = F_{Rf} = 0.167$, gray indicates cells where $F_{OD} = F_{Rf} = 2.0$ [Simulation].

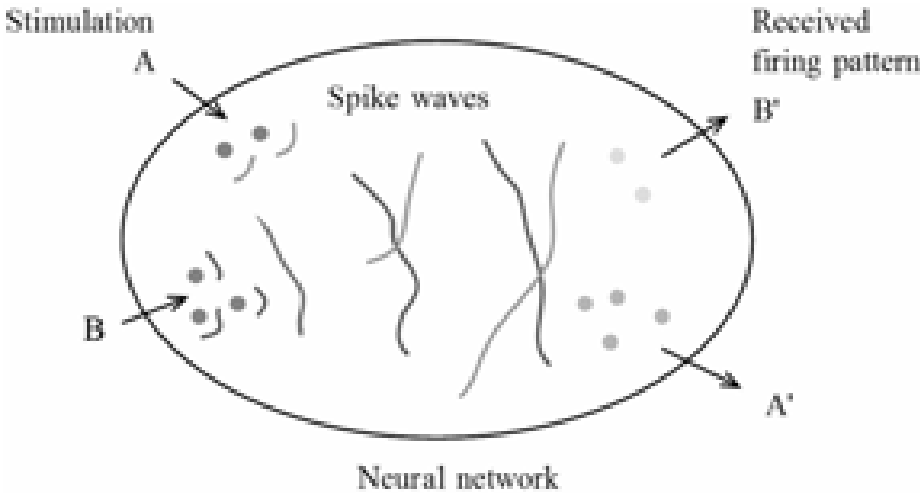

(a) Spike wave expression

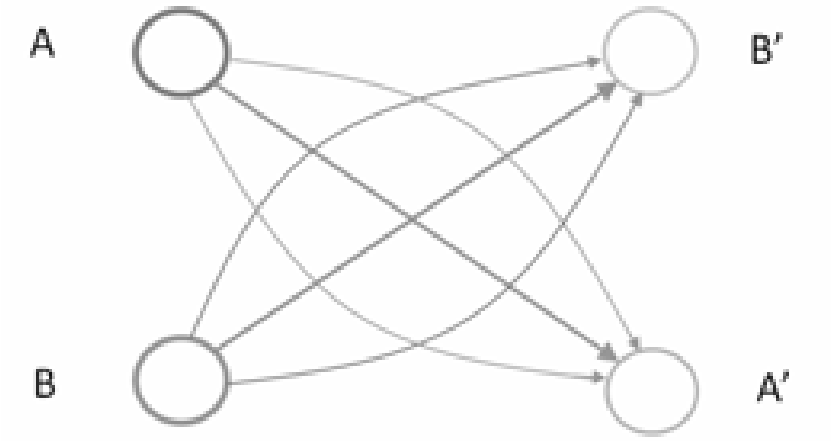

(b) Symbolic expression

Figure 6. 2:2 multiplex communication by fluctuating spike waves.

for this function, such as a series of Laplacian–Gaussian filters as employed in this section, DTW [24], interval matching [25], BPN [26] as described in the preceding section, and a non-decision method as shown in Subsection 4.8 of Section 4. However, the specific method is not essential for understanding multiplex communication.

To evaluate the capacity of networks to communicate by spike waves, we established receiving neuron groups similar to the transmitting neuron groups and devised a task in which each receiving neuron group "decides" whether a stimulus originating from a transmitting neuron group is directed to it or not based on the first four spike waves received. However, the additional heavy BPN used for this decision in the preliminary experiment did not appear realistic. Therefore, we applied a detection algorithm based on a temporal Laplacian–Gaussian (LG) function used to describe simple lateral inhibition, which is frequently observed in real neuronal networks. When the receiving neuron group $r_b = \{r_{bj}; j = 1, 2, 3\} = \{r_{b1}, r_{b2}, r_{b3}\}$ receives a spike train, it calculates the presence index (Eq. (3)) at time t from the input signal up to the fourth wave on the assumption that s_i is being stimulated (Figure 7).

$$Q_b(t) = Q_{b1}(t) + Q_{b2}(t) + Q_{b3}(t). \quad (3)$$

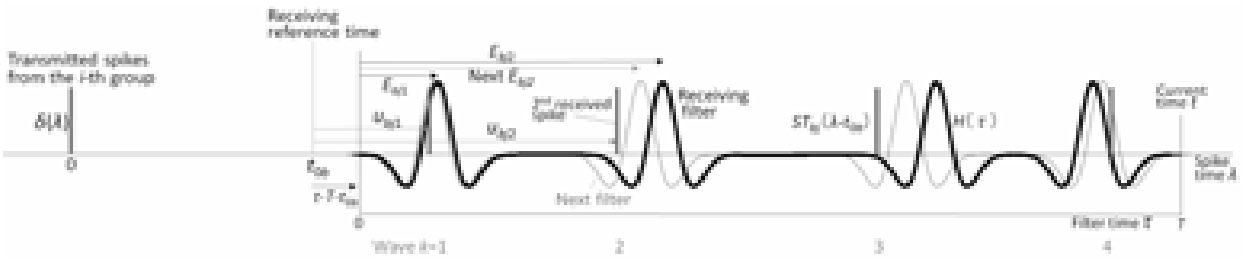

Figure 7. Detection of stimulation and learning to recognize targeted signals by the receiving neuron. The first to fourth spike waves are received at the j-th receiving neuron in the b-th receiving neuron group. Filter output is calculated as the sum of Laplacian–Gaussian weights on the received spikes. Filter shape is modified according to the received spike positions as shown by thin lines when the $b(=i)$-th neuron group fails to correctly identify stimulation from the i-th neuron group. The decreasing effect of the origin difference $t^* - T - t_{0b}$ is not shown.

Each $Q_{bj}(t)$ is calculated as the correlation between the input spike train and the filter function according to

$$Q_{bj}(t) = \int_0^T H_{bj}(\tau)\, ST_{bj}(\tau + t - T - t_{0b})\, d\tau, \quad (4)$$

where $H_{bj}(\tau)$ is a receiving correlation filter with duration T such that

$$H_{bj}(\tau) = LG(\tau - E_{bj1}) + LG(\tau - E_{bj2}) + LG(\tau - E_{bj3}) + LG(\tau - E_{bj4}) \quad (5)$$

for $b = 1,2,\ldots,C, j = 1,2,3, \tau \in [0,T]$ and

$ST_{bj}(\lambda)$ is a received spike train whose origin is t_{0b} (Figure 7) such that

$$ST_{bj}(\lambda) = \delta(\lambda - u_{bj1}) + \delta(\lambda - u_{bj2}) + \delta(\lambda - u_{bj3}) + \delta(\lambda - u_{bj4}), \quad (6)$$

where $\delta(t)$ is the Dirac delta function.

The quantity $t - T - t_{0b}$ in Eq. (4) is the shift between the origin of $H_{bj}(\tau)$ and that of $ST_{bj}(\lambda)$ at the current time t.

Then,

$$Q_{bj}(t) = LG(T - t + t_{0b} + u_{bj1} - E_{bj1}) + LG(T - t + t_{0b} + u_{bj2} - E_{bj2}) + LG(T - t + t_{0b} + u_{bj3} - E_{bj3}) + LG(T - t + t_{0b} + u_{bj4} - E_{bj4}) \quad (7)$$

for $j = 1, 2, 3,$

where

$LG(\tau)$ = Laplacian–Gaussian function = $(1 - \tau^2/\sigma^2) \exp(-\tau^2/2\sigma^2)$,

t_{0b} = Reference time at the receiving neuron group b,

u_{bjk} = Time of the k-th spike arriving (firing) at neuron r_{bj} for $k = 1, 2, 3, 4$ and

E_{bjk} = Estimated arrival time in the filter window of the k-th spike at the j-th neuron in the b-th neuron group r_b.

If each spike position u_{bjk} is well matched to the corresponding peak position E_{bjk} of the filter at time t, $Q_{bj}(t)$ is large.

Let $Q_b^* = \max_t Q_b(t)$. (8)

If neuron group i is stimulated and $Q_i^* > Q_b^*$ at the b-th receiving neuron group r_b for all $b \neq i$, then we regard the communication of channel i as successful. Otherwise, it is a failure. In C:C communication networks, this evaluation is made only from the transmitting side and not from the receiving side.

Reference time t_{0b} for the reception can be set to any time, e.g., time 1 [bin (=0.1 ms)] or the time of receipt of the first wave at the first neuron ($j = 1$) in the b-th neuron group. In asynchronous neural networks as in real neuronal networks, it is reasonable to set it to the latter because the time at which the stimulus was sent is unknown to the neurons on the receiving side.

One advantage of detection by means of a series of LG filters as opposed to the spike interval method is that interference or noise spikes occurring in irrelevant positions do not affect the filter output method [22].

2.1.4. Learning

When the communication fails, the estimated arrival time for channel i is modified, as in learning with a teacher, by

$$Updated\ E_{ijk}(L + 1) = \alpha E_{ijk}(L) + (1 - \alpha) u_{ijk}(L) \quad \text{(Learning) for } j = 1, 2, 3, k = 1, 2, 3, 4, \quad (9)$$

where α is an inertia coefficient of learning fixed at $\alpha = 0.7$ and L is the number of learning cycles. Training of the communication channels of C:C is performed cyclically (i = 1, 2,…, C, 1, 2,…, C, 1, 2,…). In the L-th learning cycle, channels i = 1, 2,…, C are trained. If the communication fails, $E_{ijk}(L)$ is updated as in Eq. (9). If communication succeeds, $E_{ijk}(L)$ is not updated.

Although there is a time difference between the filter origin and the receiving reference time t_{0b} in the early cycle, E_{ijk} approaches u_{ijk} (e.g., E_{ijk} becomes larger in Figure 7; $b = i$), the time t^* yielding the maximum value of $Q_b(t)$ is earlier (t^* becomes smaller; $t^* \rightarrow T + t_{0b}$), and the filter origin ($\tau = 0$) yielding the maximum $Q_b(t)$ approaches t_{0b} as the learning proceeds. That is, the filter axis origin (t^* - T) for peak $Q_b(t)$ approaches t_{0b} adaptively when T is large enough.

3. RESULTS

3.1. Simulation

3.1.1. Parameters

Here, σ is set to 5 (bin), which represents the permissible range of spike positions of the LG function, and bin = 0.1 [ms], corresponding to the quantization unit of time. Weights between eight neighboring neurons are assigned randomly in each trial such that the ratio of positive to negative weights is 3:1, as in typical real neurons [21]. In our model, each neuron n is characterized by two parameters, namely, output delay and refractory period. Each parameter has two characteristics, namely, the initial intrinsic characteristic (d_n and a_n, respectively; in other word "individuality") and the instantaneous characteristic (D_{nk} and A_{nk}, respectively) that varies with the firing time k.

Each neuron is an integrate-and-fire model without leakage where each neuron has random fluctuations in integration (accepting) period and output delay time, with variances represented by F_{Rf} and F_{OD}, respectively. The exact constitution of the model is not essential; rather, it is more important that each neuron has fluctuating characteristics.

3.1.2. Spatial distribution of neuron groups

As shown in Figure 8, we considered two types of neuron groups: (a) a compact group Cm and (b) a dispersed group Sp. In the simulations presented here, we used the dispersed signal source arrangement of (b) unless specified otherwise as it appeared more stable as shown below.

These two distributions were first compared for the number of learning cycles necessary to attain the first all-channel success and 10 consecutive (all-channel) successes with $F_{OD} = 0.167$ and C = 9 channels. The necessary number of learning cycles for the first success was similar and almost constant irrespective of distribution for various F_{Rf} values. However, the number of learning cycles necessary for 10 consecutive successes, regarded as an indicator that stable signal transmission channels have been established in practice, was smaller for Sp than that for Cm. This may correspond to the effects of antenna diversity and adaptive filter reception in artificial communication such as cellular base stations of mobile phones [28-31]. Thus, hereafter, we used the dispersed arrangement Sp.

3.1.3. Number of channels

Keeping the fluctuation variance of the output delay constant at $F_{OD} = 0.167$, we counted the number of learning cycles before obtaining the first (all-channel) communication success and the number necessary for 10 consecutive successes when changing the fluctuation variance of the accepting period F_{Rf} and the number of channels (Figure 9). Terms C3, C6, and C9 indicate the number of learning cycles necessary for the receiving neuron group to classify the transmitting neuron group correctly for the first time for all-channels prefixed 3, 6, and 9, respectively.

3.1.4. Fluctuation of the accepting period (F_{Rf})

The number of learning cycles necessary to attain the first success was similar for C3, C6, and C9. In other words, the number of learning cycles necessary to attain the first success was insensitive to the number of channels and the fluctuation variance in the accepting period (roughly corresponding to the refractory period) over this range. Thus, a loss of input spikes does not have a strong effect on the learning cycles needed for first success. Similarly, the number of learning cycles required before attaining 10 consecutive successes did not change markedly

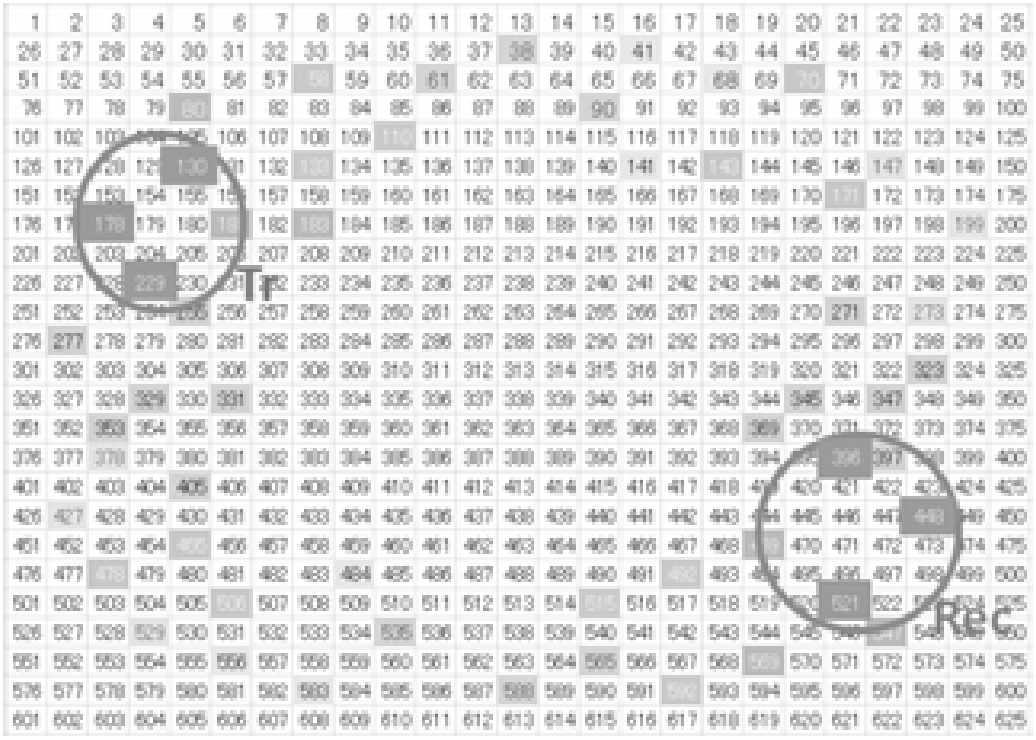

(a) Compact neuron groups: Cm

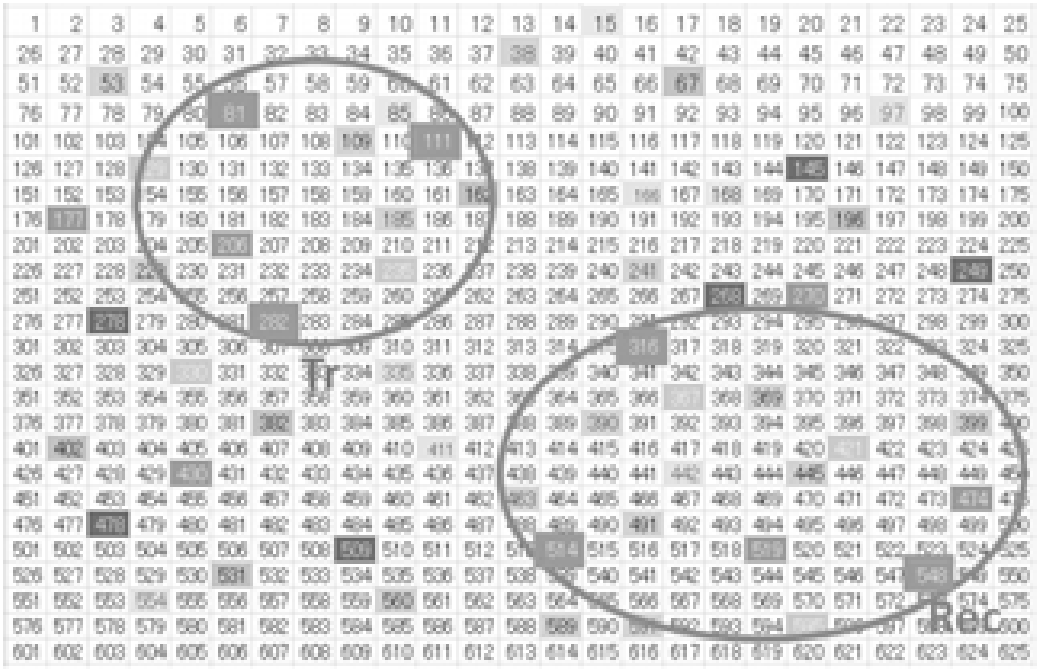

(b) Dispersed neuron groups: Sp

Figure 8. Arrangement of neuron groups for nine channels (9:9) within a 25 × 25 2D mesh neural network. Examples of a transmitting neuron group (Tr) composed of 3 neurons, a receiving neuron group (Rec) composed of 3 neurons, and other neurons in the channel groups are indicated by the same color (gray) [Simulation design].

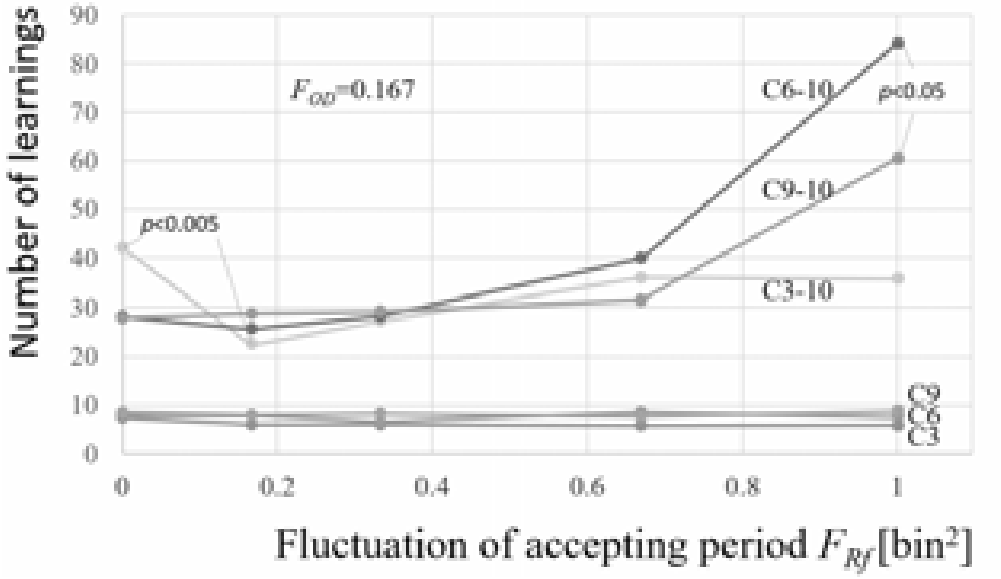

Figure 9. Number of learning cycles necessary to attain the first success (C*) and 10 consecutive successes (C*-10) when changing the variance F_{Rf} of the instantaneous fluctuation of the accepting (refractory) period. Variance F_{OD} of the fluctuation of output delay is fixed to 0.167 [bin^2] (bin = 0.1 [ms]). C = number of channels (C = 3, 6, 9) in the 25 × 25 2D mesh neural network [Simulation].

for F_{Rf} values from 1/6 (0.167) to 2/3 (0.667). However, for C3-10, the number of learning cycles required to attain F_{Rf} = 0 was significantly larger than that required for F_{Rf} = 1/6 (0.167). The reason may be as follows. We introduced fluctuations as noise, which is analogous to the effect of a support vector machine that stabilizes the classification by setting the separation hypersurface with a well margin [32]. If the fluctuation is zero, this effect cannot be expected. If several channels are set, the spike patterns of the other channels act as noise (C6-10 and C9-10) in the proper channel. For C3-10, the number of different class patterns is too small (3 − 1 = 2), and their effects are not strong enough. This may be the reason that C3-10 is significantly larger than C6-10 and C9-10 when F_{Rf} = 0. Both C6-10 and C9-10 of F_{Rf} = 1 were larger than those of F_{Rf} ≤ 2/3. This may be a direct effect of the disturbance created by the fluctuations. However, C9-10 is significantly smaller than C6-10. This may be the result of a higher number of individual training events achieved by the larger number of different channel patterns.

3.1.5. Fluctuation of the output delay (F_{OD})

Similar to variation F_{Rf}, few leaning cycles are necessary to attain the first success at different F_{OD} values. However, many learning cycles are necessary to reach 10 consecutive successes when F_{OD} is >0.2. Thus, fluctuation of the accepting period (F_{Rf}) has a weaker effect on the number of necessary leaning cycles than F_{OD}. This indicates that the loss of spikes affects the learning/ communication performance less strongly than output delay. On the other hand, increased F_{OD} decreases the success rate more strongly than increased F_{Rf} [27].

4. DISCUSSION

4.1. Background

In neuronal networks, stimulation is propagated in the form of spike trains, in which spikes are frequently lost (i.e., by failure of presynaptic spikes to elicit postsynaptic spikes). The timing of spikes also fluctuates owing to the instantaneous excitability state of the neuron. In other words, real neural networks are composed of unreliable neurons. However, these neural networks do work reliably, although it is unclear how this is achieved. To address this problem, we constructed a model using a homogeneous 2D mesh-type neural network composed of integrate-and-fire model neurons without leakage and with

fluctuating output delay and refractory (accepting) period. External stimulation is propagated asynchronously, like spike waves in a real neuronal network. The refractory period contributes to stabilizing the spike waves.

In a preliminary study, we tested a BPN for classifying the received spike waves in a 9 × 9 mesh neural network and showed that 9-point-to-1-point (9:1) communication is possible [22]. Extension of our research has been published in [27], and the essential conclusions are explained in this article.

4.2. Network shape and classification

Classification was conducted using a series of LG filters as the behavior of these filters is thought to be more physiologically plausible than BPNs. In addition, network size was extended from 9 × 9 to 25 × 25, and the behavior of the network was studied in more detail. The neural network transforms the input stimulation into seemingly random spike patterns. The BPN or the LG filter determines where the stimulus originated. In other words, neuron groups communicate by generating spike waves that are propagated like a broadcast and are recognized (using the information up to the fourth individual spike). These groups thus realize "a spatially wide area multiplex communication" that is robust against the fluctuations of relay neurons. A "spatially wide area" means that the spike waves propagate in a distributed manner via numerous relay neurons, and "multiplex communication" means that intermediate relay neurons are shared by multiple communication channels. In a preliminary study, no significant differences were found between a 2D network with connections to eight neighboring neurons and one with connections to 24 neighboring neurons which include two step-jumped connections. Therefore, the eight neighboring neuron model in this article may be enough for a basic study. Extending the network to three dimensions may further improve the robustness of multiplex communication and increase the number of possible communication channels because it will provide more possible routes between points. We conclude that multiplex communication contributes to the stability and robustness of information transmission in neural networks.

4.3. Differential effects of F_{Rf} and F_{OD}

We showed that independent signal transmission over nine channels is possible within a 25 × 25 2D mesh neural network even in the presence of response fluctuations. Fluctuations in the output delay have larger effects than fluctuations in the accepting (refractory) period on the number of learning cycles necessary to establish a communication channel and the recognition rate, possibly because, although the output delay directly affects output spike timing, only some of the spikes from neighboring neurons in the integration (accepting) period may be lost owing to fluctuations of the accepting period. In other words, loss of spikes is not as crucial for spatial multiplex communication because multiple communication routes compensate for local failures in any one transmission route. Moreover, multiplex communication also compensates for fluctuations in the spike timing of each neuron.

4.4. Effect of connection weight between neighboring neurons on learning

Connection weights between neighboring neurons were generated randomly at the beginning of each trial in the simulation. Changing weights over the course of learning may further improve classification. So far, however, we have only confirmed that the spike propagation speed is increased by Hebbian learning [33]. Considering that real networks can rapidly retrieve large amounts of randomly selected data, wave broadcasting may be employed, as in this chapter. However, the effect of learning the proper connection weights alone appears insufficient for accessing or retrieving stored information. Refer also 4.7 which describes random connections may be enough for communication.

4.5. Spatial efficiency of multiplex communication

In artificial brain chips, communication can be improved by concentrated digital synaptic switching [15], but switching connections occupy a large amount of chip space. A feasible approach to save space is to connect points via spatial multiplexing as shown in this study. Here, neurons work not only as I/O components but also

(and predominantly) as relay units for multiple communication channels. This multiuse efficiency will reduce the chip space required for communication.

4.6. Temporal multiplexing communication

We simulated only the situation where neuron groups (channels) are stimulated separately (one-by-one) and each neuron contributes to multiple communication channels (spatial multiplexing). Further studies are required to investigate the case where spikes are transmitted simultaneously over several channels and thus can mutually interfere (temporal multiplexing). In principle, a series of LG filters working asynchronously can detect target spike sequences from overlapping waves. However, this has yet to be tested experimentally.

4.7. Reservoir neural network

From the viewpoint of network form, the response of the receiving neuron group ("Network output") to the initial stimulation ("Input") is regarded as a kind of pattern transformation with random-like connections, including recurrent processing. The BPN and the LG filter function present only an additional classification process for the response of the receiving neuron group, so the network itself may be regarded as a kind of reservoir neural network [34, 35].

4.8. Effector driving

In this article, pattern classification by the neural network is examined, which is an essential function of sensory systems. However, such classification is not necessarily required to initiate a response; rather, a time series of events expressed by spatiotemporal firing patterns of neuron groups in a network may be sufficient for information processing, where events are processed causally. For example, when grasping some objects by hand, an articulated combination of muscle motions is needed. In this case, the time series of spatiotemporal firing patterns and logical and/or operational fine-tuning are required rather than classification (Figure 10).

4.9. Similarities to other communication media

Here, the spike waves from local stimulation are propagated via multiplexed communication with many neurons working as relays. This communication style is similar to that of sound transmission in the atmosphere, where receiving neurons can identify the nature of a sound source (Figure 11). It is also similar to the mobile adaptive multiple-input and multiple-output (MIMO) system developed to adapt various spatial transmission characteristics such as multi-paths using a diversity of antennae [27-30] (Figure 12). It is notable that mobile

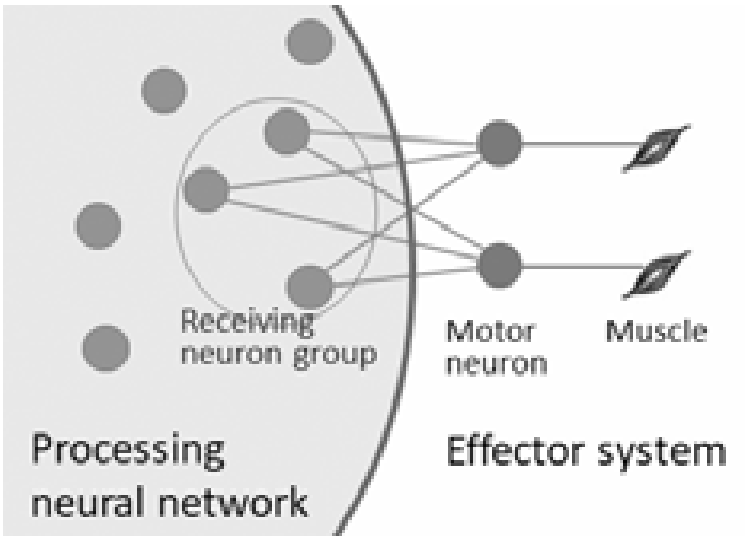

Figure 10. Synkinesis driven by a spatiotemporal pattern at a receiving neuron group. Each motor neuron can identify its own local articulated muscle contraction command by the combination of input weights.

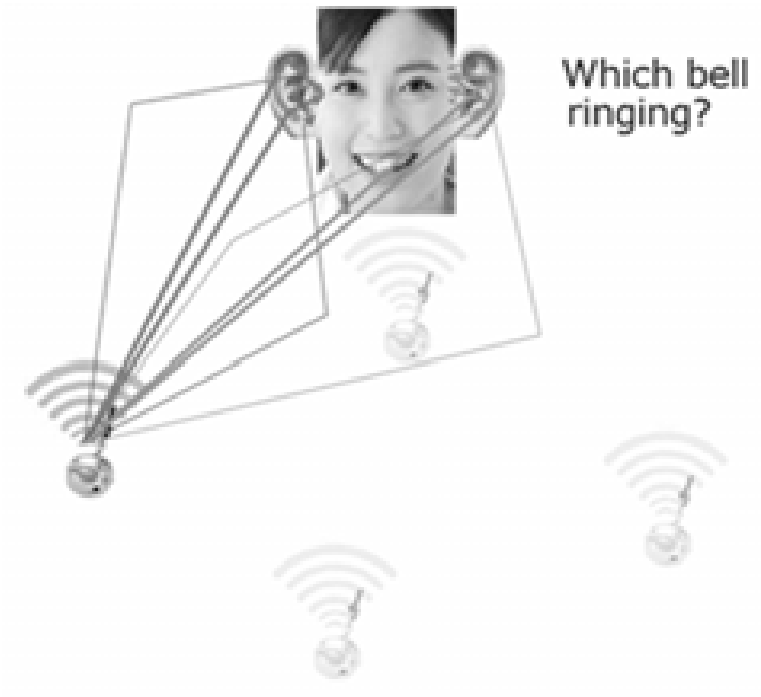

Figure 11. Sound transmission has the characteristics of multiplex communication, utilizing common space, multiple paths, and a diversity of antennae to enable identification of the source and type of sound. The neural network principle is similar to sound transmission where the receiving neuron group can identify what type of activity occurs at a remote position. The figure illustrates a 4:1 communication channel.

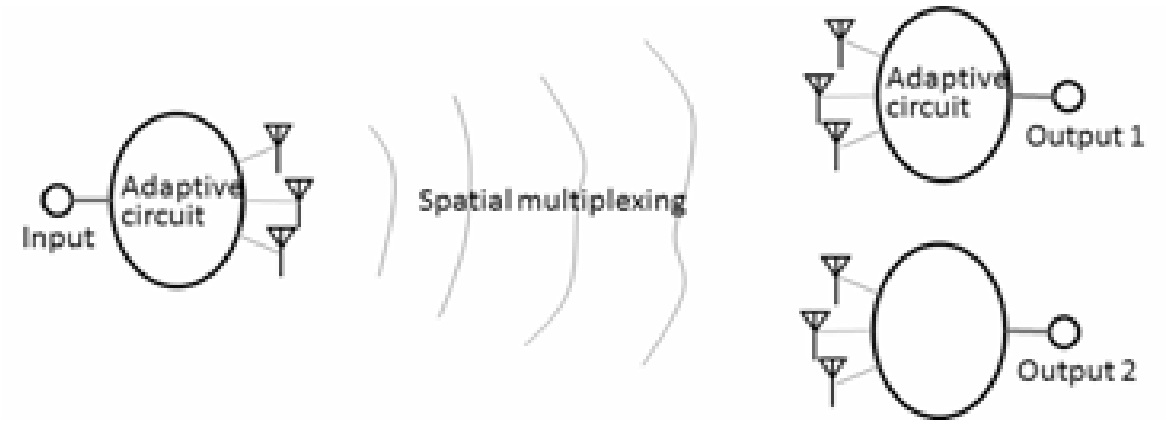

Figure 12. Mobile adaptive MIMO communication system illustrated as a 1:2 channel, suggesting that our transmitting neuron group is also extendable and can adapt to the network characteristics to enhance performance. Each station has three diversity antennae for improving performance.

communication systems have been evolving along a path resembling neural networks to compensate for different transmission media and environmental characteristics. Further, according to the concepts of MIMO, our neuron transmission groups, like receiving groups, are also extendable to allow additional adaptation to the characteristics of neural networks. Thus, we can regard multiplex communication as a general principle of neural networks.

4.10. Robustness by multiplex communication

In our flat-type 2D mesh neural network, losing spikes did not significantly impair communication owing to the effects of the multiplexing. This appears consistent with recent findings from deep learning research showing that low-precision calculations, neglect of small value weights, and grouping (pooling) still achieve robust processing. Rather than local reliability of transmission between points, neural networks achieve total robustness by utilizing redundant connections.

4.11. Effect of music for synchronization

The communication system described here needs some local and global synchronization or timing measures in the network explicitly and implicitly. However, microscopically the neural network contains many loops which will function as a self-oscillation circuit with relatively unstable or variable frequency. Therefore, it should be important to keep synchronization within communication range.

On the other hand, most people are fond of music. There should be some positive reasons to seek for music and dance. The effects of music are studied a lot [36] from macroscopic view especially from the relation between body and music. Physical pendulum-like motion and music give stable rhythm and tempo as well as frequency of music instruments, and it may be effective to keep and train the synchronization among micro level neural network.

Our neuron model neglected the threshold value to fire. However, it may be reasonable to assume that if the environmental electrical potential value such as global brain wave is changed, the characteristics of the neuron such as refractory period and output delay time will be varied through the threshold. It is also observed that there is a certain tendency of neurons firing continuously even after stopping the repetitive stimulations [37]. That is, there is a possibility that the music and dance contribute to the synchronization as outside clock for communication within the neuronal network of human and animals.

4.12. Correspondence to wet experiment: Bridging to Part 2 (the succeeding article [23])

A central feature of our research is the parallel evaluation of in silico simulations and recordings from real neuronal networks. The correspondence between simulations and multi-electrode extracellular recordings is explained in the following subsections [21].

4.12.1. Neuron characteristics and distribution under electrodes

It is challenging to record action potentials (spikes) from individual neurons using extracellular electrodes as most will detect multiple spikes from several (m) proximal neurons (Figure 13).

Figure 14 shows an example of a spike train measured at each of 64 electrodes (in an 8 × 8 array) from a real neuronal network. Although these look like random sequences, they are often pseudo-random code-like sequences. For example, we can observe the sequence “1101” (closed ellipse; code no. 1) or “1011” (ellipse with top crack; code no. 2) which are core components of M-sequences “1101000” and “1011000,” respectively [38].

4.12.2. Model of multi-electrodes on a 2D mesh neural network

A multi-electrode array is modeled in Figure 15, where each electrode detects the activity of several local neurons. An example output of an individual electrode is shown in Figure 16. The response varies according to the number of detected neurons. We can also observe a code “1011,” which is a representative of the M-sequence family. Since there are many loop circuits such as shift register-like circuits along the spike pathway, many pseudo-random sequences like M-sequence are generated as shown in Figure 17.

4.12.3. Code flow

Figure 18 presents pseudo-color image sequences depicting detected codes “1101” and “1011” from Figure 14 (movies are available through our website). These movies reveal that codes are flowing from the first (stimulus) electrode to the neighboring electrode without markedly changing shape. This is confirmed by statistically comparing the codes to those from shuffled and random spike trains [20]. However, correlations of the detected codes gradually decrease with time and spatial distance. Thus, the code can be used to track the flow of spikes or signals.

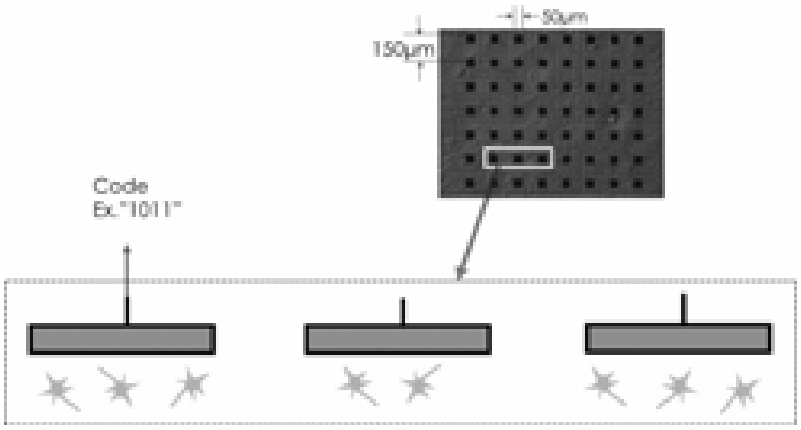

Figure 13. (Upper) Micrograph of cultured hippocampal neurons of a Wistar rat in a microelectrode array. Black rectangles indicate electrodes. (Lower) Illustration of a vertical section. Each electrode catches spikes from several neurons. We can observe spike trains containing code such as "1011". Each bit ("1" or "0") is considered from different neurons for short time length (short bit-width) code, since it takes more time for the same neuron to fire twice than the refractory period or observing window period [20] [Set up of wet experiment].

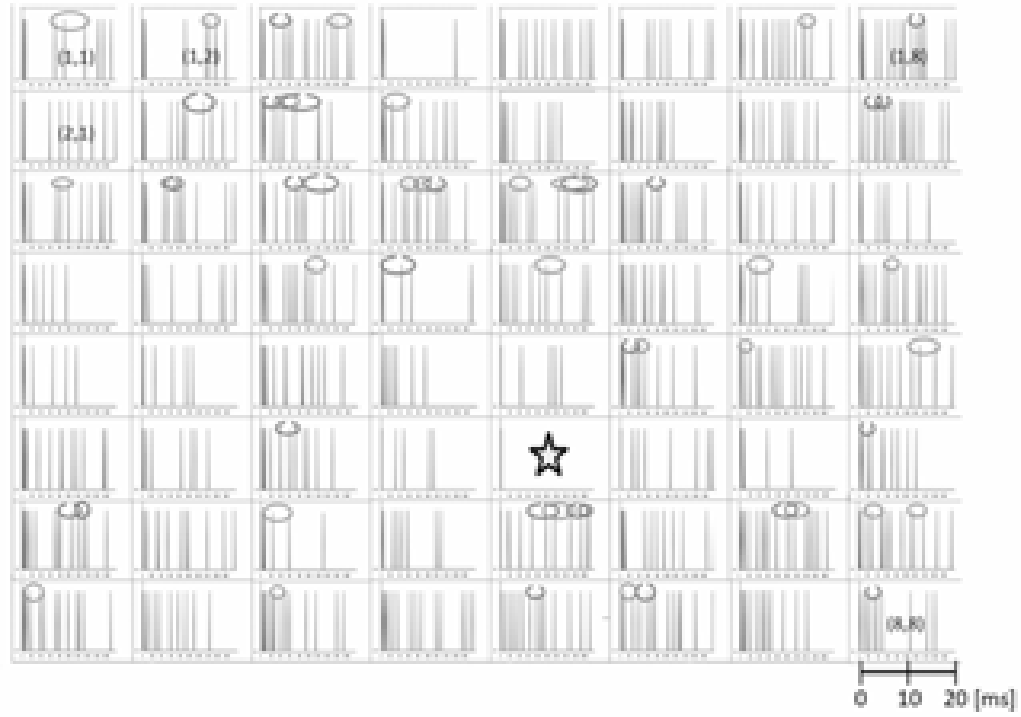

Figure 14. Examples of spike trains recorded from a real neuronal network using 8 × 8 multi-electrodes. The recording period was between 0 and 18 [ms] (horizontal axis) after the stimulation pulse was delivered (at time 0) from the electrode marked with a star [20]. The ellipse with top crack shows the code "1011," and the closed ellipse shows "1101, with each having a bit of width more than 0.6 [ms]. In the simulation, spike of each neuron can be identified. On the other hand, in the wet experiment of this figure, since there are multiple neurons within each electrode response area, spikes from different neurons cannot be distinguished. However, since the measurement period is shorter than the expected refractory period (accumulation time; about 7 [ms], 70 [bins]), the number of spikes measured from the same neuron is usually at most one. Thus, almost all spikes arise from different neurons [Wet experiment].

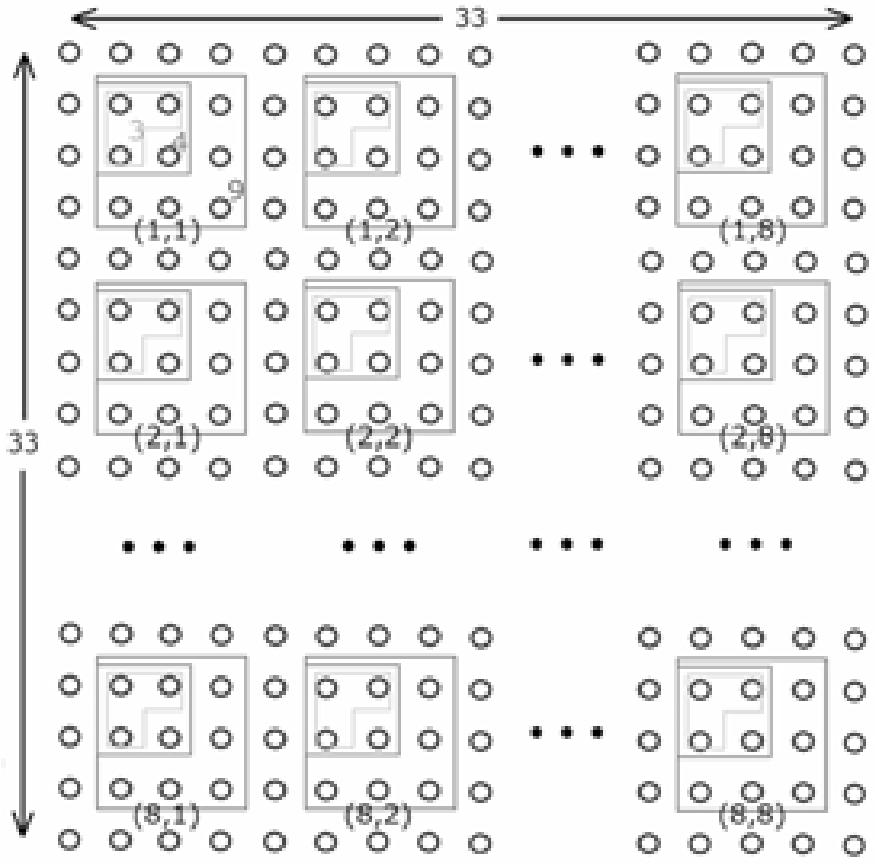

Figure 15. Arrangement of 8 × 8 multi-electrodes [(1, 1), (1, 2),…, (8, 8)] on a simulated 33 × 33 2D mesh neural network. Each electrode acquires spikes of two to nine neurons. For example, figure "9" showing 3 × 3 block of neurons (○) indicated with (1, 1) shows that electrode (1, 1) collects spikes from nine neurons (covering number is 9). In addition, figures "3" and "4" are likewise; "2" and "5"–"8" are not shown. Connections between eight neighboring neurons are randomly generated with given stochastic characteristics [Simulation design].

4.12.4. Code spectrum

From 120 pseudo-random-like sequences, we selected 21 major (frequently occurring) codes of length less than 8 (bins with or without a spike indicated as 1 or 0) and having a spike at the beginning and end. Figure 19 shows an example of how many codes appear from the 63 non-stimulating electrodes according to the refractory period a_0, ratio of positive to negative weights c, and number of neurons m detected by the electrode. We call these curves (S_m) "code spectra," and they can be used as functions to decompose an observed spectrum. In the simulation, time is segmented into bins of 0.1 [ms], and the accepting period corresponding to integration time or equivalently refractory period is set to 20-80 bins (2-8 [ms]).

4.12.5. Estimation of parameters and covering number

By fitting the simulation to multi-electrode recordings from real neuronal networks, we can estimate a_0, c, and the distribution Prob(m) of how many neurons (m) each electrode detects (covers), such that

$$\text{Squared estimation error } (a_0, c, \{\text{Prob}(m)\}) = \|\boldsymbol{S} - \hat{\boldsymbol{S}}\|^2 \quad (10)$$

is minimized, where

$$\hat{\boldsymbol{S}}\,(a_0, c, \{\text{Prob}(m)\}) = \sum_{m=2}^{9} \text{Prob}(m)\,.\,\boldsymbol{S}_m\,(a_0, c)$$

(Estimated code spectrum) (11)

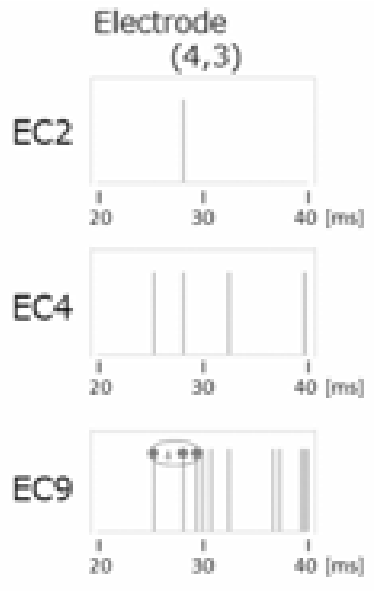

Figure 16. An example of simulated measurement from an electrode EC*m* when changing the covering number (*m*) of neurons at position (4, 3) after the stimulation. Circles ● and triangle **Δ** correspond to "1" and "0" of the pseudo-random code "1011," respectively. Horizontal axis shows the elapsed time after the electrode (1, 4) was stimulated [Simulation].

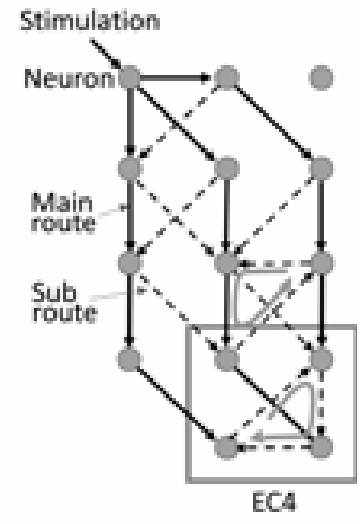

Figure 17. Stimulation added to top of the left-hand-side neuron is propagated along the main route with high weights (solid lines) to electrode EC4. However, it propagates also on the sub-routes, including loops. Then, the original stimulation is propagated as repeating spike waves through main routes as well as sub-routes. Since the routes include loops as shown with closed loop arrow, pseudo-random codes are often observed within the repeating spike waves.

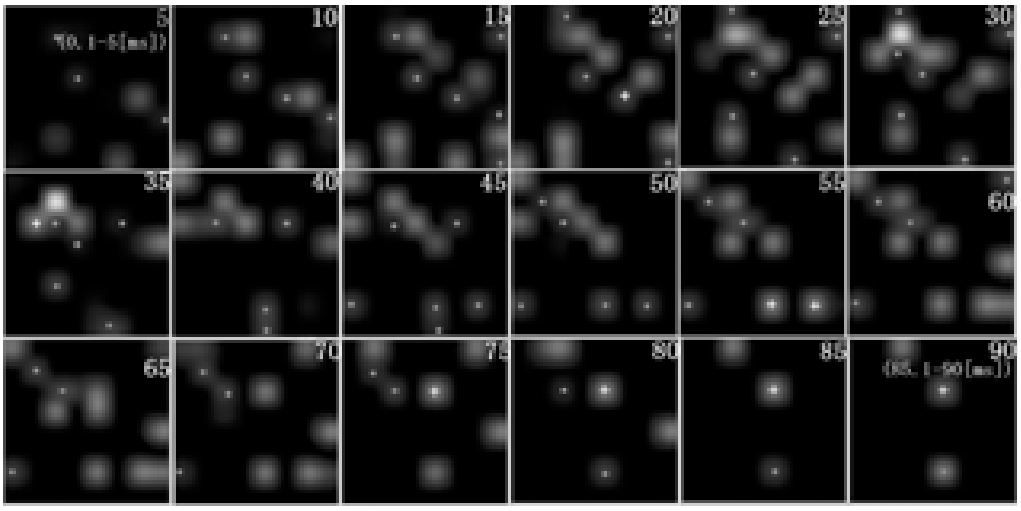

Figure 18. Serial images of the simple pseudo-random sequences (code) "1011" (spot with white '•'), "1101" (spot without mark), and both superimposed (spot with "+") observed at each electrode of an 8 × 8 channel array underlying a cultured neuronal network. Bit lengths are 0.6-3.0 [ms], and the time of post stimulation is shown at the top right of each panel.

Moving color images of these patterns are available at 'http://www.nbl-technovator.jp/NBL_Tech/paper/CodeFlowFig8.pdf'
From these serial images, it can be seen that the codes are flowing without substantially changing shape from the first (stimulation) electrode to one of the eight neighboring electrodes and then to one of the further neighboring electrodes. We can confirm this signal preservation statistically by comparison to shuffled and random sequences [Wet experiment].

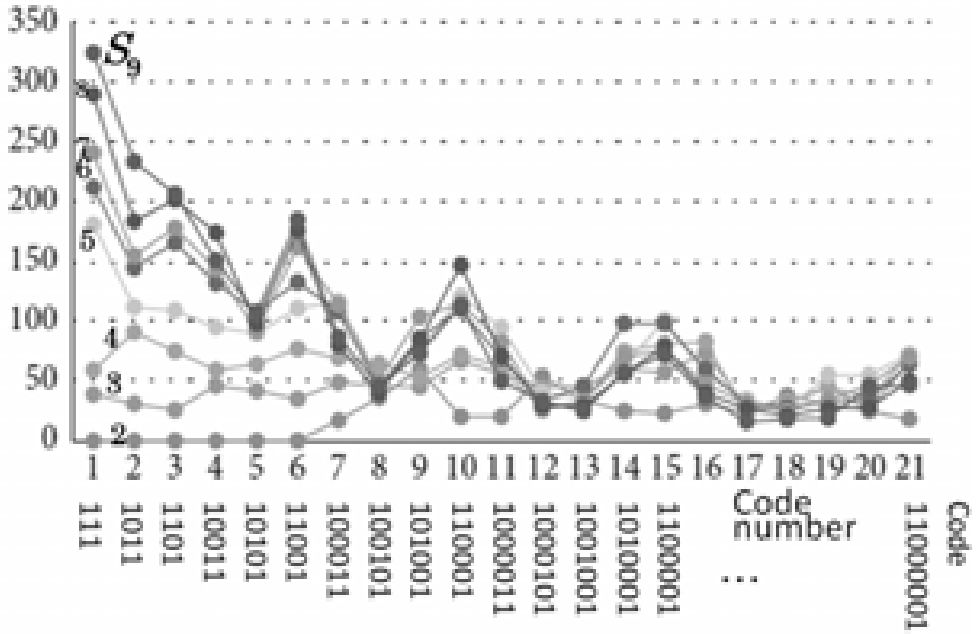

Figure 19. Example of code spectrum components S_m for several parameters of accepting period (refractory period) a_0 = 10 and positive and negative weight balance c = 1. The horizontal line represents code numbers (1, 2,…, 21), whose number of "1" in the code is 3. That is, code 1 = "111," code 2 = "1011," code 3 = "1101," code 4 = "10011," code 5 = "10101,"…, code 21 = "11000001" [22]. The vertical line represents the total number of codes detected during the first 200 [ms] after stimulation (2000 time bins of 0.1 [ms/bin]) and from 63 electrodes [Simulation].

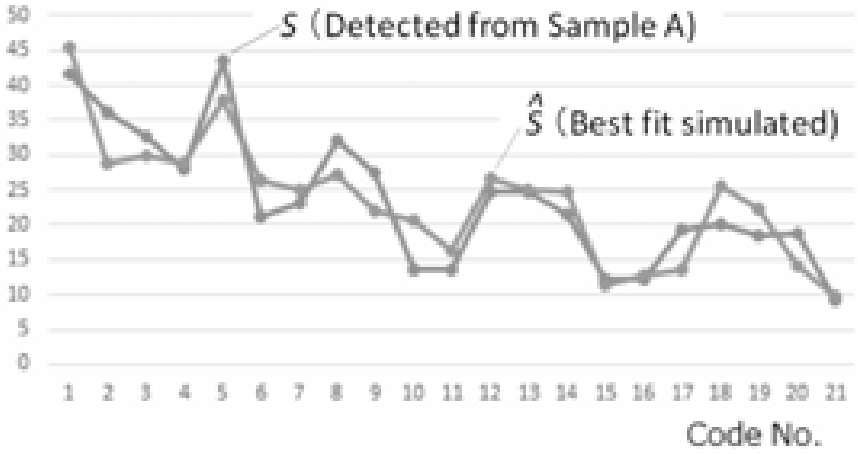

Figure 20. Fitting of simulated code spectrum $\hat{S}$ to spectrum S derived from nine trial measurements of real culture neuronal networks ("Sample A"). The curve S shows the average number of individual spike train codes over nine trials detected from 63 non-stimulating electrodes in 200 [ms] following stimulation expressed in 2000 time bins of 0.1 [ms]. The bit width of the code is 0.6-2.0 [ms] (6-20 [bins]). In principle, codes are detected with 1% time accuracy, although the accuracy is reduced (round error) by a considerable percentage because of the minimum unit of 0.1 [ms]. This curve can be considered a "signature" of spike trains. The curve $\hat{S}$ derived from simulations is the best fit to the real code spectrum. We obtained estimated a_0 = 8 [ms], c = 2.5, and S_m probability distribution (Prob(2), Prob(3),…, Prob(9)) = (0.3, 0.1, 0, 0, 0, 0.05, 0, 0.55), with a normalized RMS error of 0.179. Consequently in this case, it is estimated that more than half will be $m \geqq 9$, and 30% will be m = 2, that is, there seems to be large variations of neuron density [Simulation and wet experiment].

$$\sum_{m=2}^{9} \text{Prob}(m) = 1 \text{ (Constraint)} \quad (12)$$

as shown in Figure 20. Code spectrum $\boldsymbol{S}$ and component code spectrum $\boldsymbol{S}_m$ are expressed as E and E_m, respectively, in [21]. Since few spikes are included in $\boldsymbol{S}_m$ for $m = 1$, $\boldsymbol{S}_1$ is not included in the above calculation.

4.12.6. Possibility of connection analysis

The above (4.12.4) shows the adequateness of our network model composed of integrate-and-fire model neurons (a) without leakage, (b) with a fluctuating refractory period and output delay, and (c) organized as a homogeneous flat 2D mesh-type network, as well as (d) a multi-electrode model that detects spikes from multiple neurons per electrode channel. These techniques may be applicable for the analysis of neuronal circuits around electrodes.

4.12.7. 2:n communication on cultured neuronal network

In Part 2 [23], communication was examined in cultured neuronal networks to complement and confirm the *in silico* findings of Part 1 (this article). Figure 21 shows the best data for 2:*n* communication in a cultured neuronal network [26]. At 32 of 62 electrodes (gray), we could identify the received spikes as originating from stimulus electrode "1" or "2" with significant accuracy, and hence there was substantial correspondence between *in silico* results in Part 1 and real neuronal network recordings in Part 2.

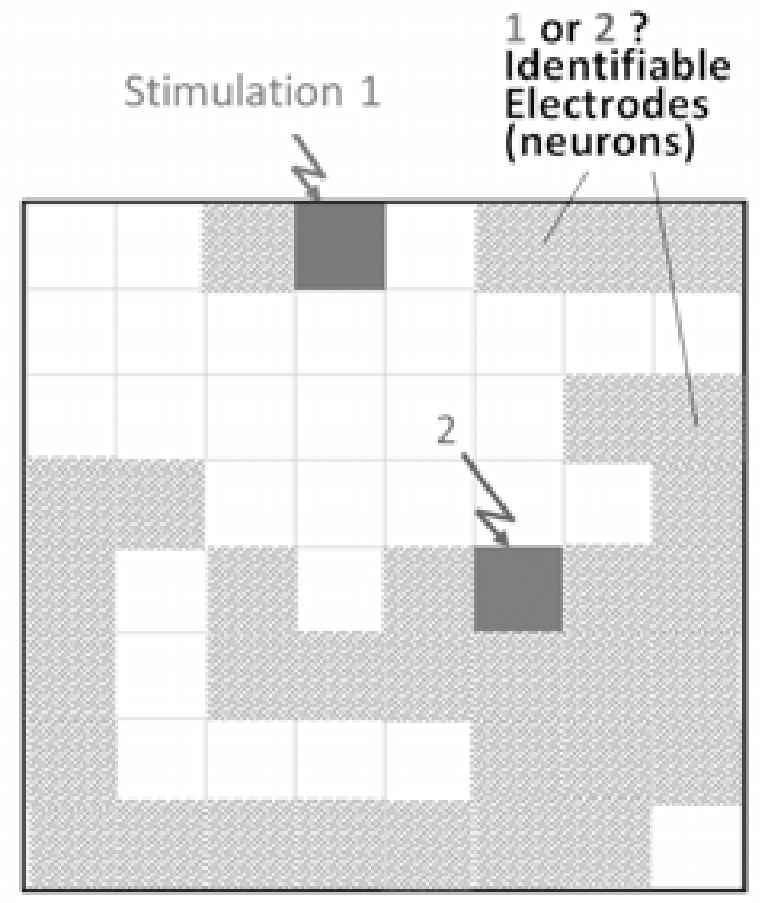

Figure 21. The best data for 2:*n* communication within a neuronal network cultured on a 8 × 8 multi-electrode [26]. Overall, 32 of 62 electrodes (52%) could identify received spikes as originating from stimulation electrode "1" or "2" with significant accuracy [Wet experiment].

5. CONCLUSION

The main conclusions of this paper, including those from preliminary results published previously, can be summarized as follows.

(1) To our knowledge, these studies are the first to simulate asynchronous multiplex communication in a neural network. Our work reveals a signal transmission principle in neural networks that may resolve the problem of reliable neural communication among neurons with fluctuating transmission characteristics, including spike failures.

(2) Simulation results were in good agreement with recordings from real 2D neuronal networks [24-26, 37] examining 2:1 and 2:2 communication as well as with preliminary results examining 3:1 and 3:3 communications.

(3) Simulations demonstrated quantitatively that group firing or synchrony of neurons, as is frequently observed in real neuronal networks [39-41], facilitates stable information transmission even with spike fluctuations at the single neuron level.

(4) Neurons function in most instances as relays in multiple communication pathways.

(5) Multiplex communication promotes stable and robust transmission in spite of the fluctuating characteristics of individual neurons by using a spatially distributed range of neurons as relays.

(6) Multiplex communication may reduce the ample space required for switching connections in artificial brain circuits.

(7) We show that the communication mode of neural networks is similar to that used to identify sound sources by ears and high-performance mobile communication using adaptive filter reception and a diversity of antennae.

(8) We explain the reasonable correspondence between simulations in Part 1 and *in vitro* experiments on cultured neuronal networks in Part 2.

(9) These findings may provide a foundation for the development of brain-machine or even brain-brain interfaces.

ACKNOWLEDGEMENTS

This work was supported in part by Grants-in-Aid for Scientific Research of Exploratory Research JP21656100, JP25630176, JP16K12524, JP17K20029, and Scientific Research (A) JP22246054 of the Japan Society for the Promotion of Science. The author is also grateful to Dr. Yoshi Nishitani of Osaka University, Prof. Chie Hosokawa of Osaka City University, Prof. Yuko Mizuno-Matsumoto of University of Hyogo, Dr. Tomomitsu Miyoshi of Osaka University, and Prof. Yen-Wei Chen of Ritsumeikan University for supporting the research.

CONFLICT OF INTEREST STATEMENT

To the best of the author's knowledge, there is no conflict of interest, financial or otherwise.

REFERENCES

1. Cessac, B., Paugam-Moisy, H. and Viéville, T. 2010, J. Physiol. Paris, 104, 5.
2. Tyukin, I., Tyukina, T. and Leeuwen, C. 2009, Neural Networks, 22, 425.
3. Mohemmed, A., Schliebs, S., Matsuda, S. and Kasabov, N. 2013, Neurocomputing, 107, 3.
4. Olshausen, B. A. and Field, D. J. 1996, Nature, 381, 607.
5. Bell, A. J. and Sejnowski, T. J. 1997, Vision Res., 37, 3327.
6. Tamura, S., Mizuno-Matsumoto, Y., Chen, Y. W. and Nakamura, K. 2009, The Fifth Int'l Conf. Intelligent Information Hiding and Multimedia Signal Processing (IIHMSP2009), Y. W. Chen (Ed.), IEEE, Boca Raton, A10-07(No.546).
7. Abeles, M. 1982, Local Cortical Circuits: An Electrophysiological Study, Springer, Berlin.
8. Abeles, M. 2009, Scholarpedia, 4, 1441. http://www.scholarpedia.org/article/Synfire_chains
9. Izhikevich, E. M. 2006, Neural Comput., 18, 245.
10. Perc, M. 2007, Chaos Solitons Fractals, 32, 1118. doi:10.1016/j.chaos.2005.11.035.
11. Zhang, H., Wang, Q., Perc, M. and Chen, G. 2013, Commu. Nonlinear Sci. Numerical Simul., 18, 601.
12. Nishitani, Y., Hosokawa, C., Mizuno-Matsumoto, Y. Miyoshi, T., Sawai, H. and Tamura, S. 2012, Comput. Intell. Neurosci., Article ID 862579. doi:10.1155/2012/862579.

13. Iguchi, T., Hirata, A. and Torikai, H. 2010, IEICE Trans. Fundamentals, E93-A, 1486.
14. Srinivasa, N. Zhang, D. and Grigorian, B. 2014, IEEE Trans. Neural Netw. Learn. Syst., 25, 585.
15. Merolla, P. A., Arthur, J. V., Alvarez-Icaza, R., Cassidy, A. S., Sawada, J., Akopyan, F., Jackson, B. L., Imam, N., Guo, C., Nakamura, Y., Brezzo, B., Vo, I., Esser, S. K., Appuswamy, R., Taba, B., Amir, A., Flickner, M. D., Risk, W. P., Manohar, R. and Modha, D. S. 2014, Science, 345, 668. doi:10.1126/science. 1254642
16. Mizuno-Matsumoto, Y., Okazaki, K., Kato, A., Yoshimine, T., Sato, Y., Tamura, S. and Hayakawa, T. 1999, IEEE Trans. Biomed. Eng., 46, 271.
17. Mizuno-Matsumoto, Y., Ishijima, M., Shinosaki, K., Nishikawa, T., Ukai, S., Ikejiri, Y., Nakagawa, Y., Ishii, R., Tokunaga, H., Tamura, S., Date, S., Inouye, T., Shimojo, S. and Takeda, M. 2001, Brain Topography, 13, 269.
18. Tamura, S., Nishitani, Y., Kamimura, T., Yagi, Y., Hosokawa, C., Miyoshi, T., Sawai, H., Mizuno-Matsumoto, Y. and Chen, Y-W. 2013, Auto. Control Intell. Systems, 1, 121. doi:10.11648/j.acis.20130106.11.
19. Kamimura, T., Yagi, Y., Tamura, S. and Chen, Y. W. 2015, Auto. Control Intell. Systems, 3, 63. doi:10.11648/j.acis.20150305.11
20. Tamura, S., Nishitani, Y., Hosokawa, C., Miyoshi, T., Sawai, H., Kamimura, T., Yagi, Y., Mizuno-Matsumoto, Y. and Chen, Y. W. 2016, Comput. Intell. Neurosci., Article ID 7267691. doi:10.1155/2016/7267691
21. Tamura, S., Nishitani, Y., Hosokawa, C., Miyoshi, T., Sawai, H. 2016, Comput. Intell. Neurosci., Article ID 7186092. doi:10.1155/2016/7186092
22. Tamura, S., Nishitani, Y. and Hosokawa, C. 2016, AIMS Neuroscience, 3, 385. doi: 10.3934/Neuroscience.2016.4.385
23. Nishitani, Y. 2020, Curr. Tren. Neurol., 14, 35.
24. Nishitani, Y., Hosokawa, C., Mizuno-Matsumoto, Y., Miyoshi, T., Sawai, H. and Tamura, S. 2016, Int. J. Academ. Res. Reflect., 4, 11.
25. Nishitani, Y., Hosokawa, C., Mizuno-Matsumoto, Y., Miyoshi, T. and Tamura, S. 2017, AIMS Neuroscience, 4, 1. doi: 10.3934/Neuroscience.2017.1.1.
26. Nishitani, Y., Hosokawa, C., Mizuno-Matsumoto, Y., Miyoshi, T. and Tamura, S. 2018, AIMS Neuroscience, 5, 18. doi: 10.3934/Neuroscience.2018.1.18.
27. Tamura, S., Nishitani, Y., Hosokawa, C. and Mizuno-Matsumoto, Y. 2019, IEEE Trans. Neural Netw. Learn. Syst., 30, 2336. doi: 10.1109/TNNLS.2018.2880565
28. Vaughan R. G. and Andersen, J. B. 1987, IEEE Trans. Veh. Technol., 36, 140. doi: 10.1109/T-VT.1987.24115
29. Zheng L. and Tse, D. N. C. 2003, IEEE Trans. Inform. Theory, 49, 1073.
30. Ge, S. S. and Wang, C. 2004, IEEE Trans. Neural Networks, 15, 674.
31. Larsson, E. G., Edfors, O., Tufvesson, F. and Marzetta, T. L. 2014, IEEE Communications Magazine, 52, 186.
32. Suykens, J. A. K. and Vandewalle, J. 1999, Neural processing letters, 9, 293.
33. Sakuma, S., Mizuno-Matsumoto, Y., Nishitani, Y. and Tamura, S. 2017, AIMS Neuroscience, 4, 238. doi:10.3934/Neuroscience.2017.4.238.
34. Lukoševičius M. and Jaeger, H. 2009, Computer Science Review, 3, 127.
35. Duport, F., Smerieri, A., Akrout, A., Haelterman, M. and Massar, S. 2016, Scientific Reports, 6, Article number 22381.
36. Todd, N. P. M. Fall 1999, Music Perception, 17, 115. doi: 10.2307/40285814
37. Nishitani, Y., Hosokawa, C., Mizuno-Matsumoto, Y., Miyoshi, T. and Tamura, S. 2019, AIMS Neuroscience, 6, 240. doi: 10.3934/Neuroscience.2019.4.240
38. Golomb, S. W. and Gong, G. 2005, Signal Design for Good Correlation: For Wireless Communication, Cryptography, and Radar, Cambridge University Press, Cambridge, England.
39. Perc, M. 2005, Physical Rev. E, 72, 1. doi: 10.1103/PhysRevE.72.016207.
40. Havenith, M. N., Yu, S., Biederlack, J., Chen, N. H., Singer, W. and Nikolić, D. 2011, J. Neurosci., 31, 8570.
41. Sakurai, Y. and Takahashi, S. 2013, Europ. J. Neurosci., 37, 623. doi:10.1111/ejn.12070.